PHYSICAL REVIEW E **75**, 060501(R) (2007)

Induced dipoles and dielectrophoresis of nanocolloids in electrolytes

Sagnik Basuray and Hsueh-Chia Chang*
Center for Microfluidics and Medical Diagnostics, Department of Chemical and Biomolecular Engineering, University of Notre Dame, Notre Dame, Indiana 46556, USA

(Received 15 March 2007; published 25 June 2007)

Electric induced dipoles of nanocolloids the size of the Debye length are shown to be one order stronger than predicted by the classical Maxwell-Wagner theory and its extensions. The difference is attributed to normal ion migration within the diffuse layer, and adsorption onto the Stern layer at the poles. The characteristic relaxation frequency (the crossover frequency for dielectrophoresis) is shown to be inversely proportional to the *RC* time of the diffuse layer capacitance and resistance, and has an anomalous −1 scaling with respect to the product of the Debye length and the particle size.

DOI: 10.1103/PhysRevE.75.060501 PACS number(s): 82.45.−h, 47.57.jd, 47.65.−d, 66.10.Ed

Dielectrophoresis (DEP) has become an increasingly popular means of manipulating and identifying immunocolloids, bioparticles, and DNA molecules in microfluidic devices [1–3]. The dielectrophoretic force on the particle results from induced ac particle dipoles, which can develop by either conductive or dielectric polarization mechanisms according to classical Maxwell-Wagner (MW) theory [2]. For conducting particles with low permittivity, conductive polarization dominates at low frequency and dielectric polarization at high frequency, with opposite dipole orientations with respect to the applied field and opposite positive (toward high field) and negative (toward low field) DEP mobility. As the length of both the particle capacitor and the resistor is the particle size a, the dipole orientation and RC relaxation time, as determined by $f_{c.m.}=(\tilde{\varepsilon}_P-\tilde{\varepsilon}_M)/(\tilde{\varepsilon}_P+2\tilde{\varepsilon}_M)$, the Clausius-Mossotti factor, is size independent. The complex permittivity $\tilde{\varepsilon}$ is related to the real permittivity ε and conductivity σ via the ac field frequency ω for both particle (P) and medium (M). Hence, there exists a crossover frequency ω_{CO}, defined by $\mathrm{Re}[f_{c.m.}]=0$, when the induced dipole vanishes, which the MW theory predicts to be size independent:

$$\omega_{MW}=\frac{1}{2\pi}\sqrt{\frac{(\sigma_P-\sigma_M)(\sigma_P+2\sigma_M)}{(\varepsilon_M-\varepsilon_P)(\varepsilon_P+2\varepsilon_M)}}. \quad (1)$$

This MW theory was recently found to be inaccurate for nanocolloids [3–6]. The ω_{CO} data of Green and Morgan [6] in Fig. 1 for nanosized latex particles clearly show a particle size dependence. In fact, according to the classical MW theory Eq. (1), latex particles with permittivity and conductivity both lower than the medium are not expected to exhibit any crossover phenomenon. Ermolina and Morgan [7] have suggested that, for latex and other particles with negligible native conductivity, σ_p should be dominated by Stern and diffuse layer conduction effects, as described by the classical theories for electrophoresis, (see the review in [8]). With negligible native conductivity, the corrected particle conductivity becomes $\sigma_p=(2K_s/a)+(2K_D/a)$, where K_s is the Stern layer conductance and K_D the diffuse layer conductance, which includes a dependence on the particle ζ potential due to osmotic flow effects. However, that the effective conductance is the sum of the two conductance contributions from the Stern and diffuse layers reflects the implicit assumption in the classical theories that the conduction "surface" currents are tangential. This is true for the Stern layer, which is always thin compared to the particle, and hence its internal field is always tangential to the latex insulator particle. It is, however, inaccurate for diffuse layers with Debye length $\lambda=(\varepsilon_M D/\sigma_M)^{1/2}$ (D is the ion diffusivity) comparable to a. With the normal length scale comparable to the tangential one in such thick layers, the normal field and current become important in the diffuse layer, and this effect is not captured by the classical theories. Moreover, modeling just conduction (electromigration) in the diffuse layer is inadequate, as the neglected diffusive flux can counter electromigration to produce tangential equilibrium or Poisson-Boltzmann distribu-

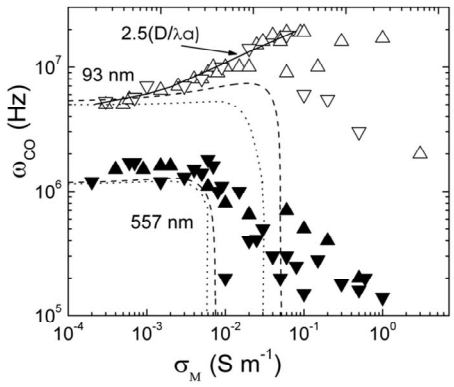

FIG. 1. Green and Morgan's [6] crossover frequency data for 557 (black triangles) and 93 nm (unfilled triangles) latex particles. The classical MW theory with a conducting Stern layer is shown as a dotted line. The Stern layer conductance is 1.46 nS for 93 nm particles and 1.92 nS for 557 nm particles, calculated from the data asymptote at low medium conductivity. The dashed line is from an extended theory of [7] that includes tangential conduction in the diffuse layer (with the same surface conductance as ours and ζ potential of 67 mV for 93 nm and 45 mV for 557 nm particles from Fig. 5 of [7]). The solid line corresponds to the scaling theory of Eq. (2) with a scaling constant of 2.5 and $D=5\times10^{-9}$ m^2/s.

*Author to whom correspondence should be addressed. hchang@nd.edu

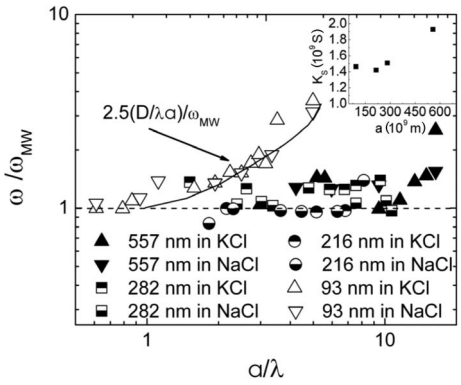

FIG. 2. Scaled data of Green and Morgan for four different latex particle dimensions in different KCl and NaCl electrolytes with $D=5\times10^{-9}$ m^2/s to resolve the data points across a wide range of λ/a. The Stern layer conductance using the data asymptote at low conductivity for different particle sizes is shown as the inset. The scaling theory of Eq. (2) captures the anomalous rise of the 93 nm data when $\lambda\sim a$.

tions. We hence expect the improved MW theories to be valid only at lower conductivity when $\lambda\gg a$, or for large particles, $a\gg\lambda$.

At the limit of infinitely low medium conductivity, the Stern layer conduction contribution dominates that from the diffuse layer even in these theories, and the crossover frequency with negligible native permittivity approaches $\omega_\infty=1/2\pi(K_s/\sqrt{2}a\varepsilon_M)$. Using this limiting value for the particle data of Green and Morgan [6] to estimate K_s for different particle sizes (see inset of Fig. 2), the MW theory with Stern layer conduction (dotted curve) is shown in Figs. 1 and 2 for various particle sizes. It is shown to accurately capture the measured crossover frequencies of large particles, but still fails to describe the data for nanocolloids with smaller dimensions, at medium conductivities corresponding to $a\sim\lambda$, as shown in Fig. 1. Although this new crossover frequency is size dependent, it falls monotonically with respect to the medium conductivity, instead of exhibiting the order-of-magnitude rise for the smaller particle (93 nm). The dashed curve in Fig. 1 corresponds to the extended theory, which includes diffuse layer conduction and electro-osmotic flow convection. Using ζ potential estimates from Fig. 5 of [7] for all latex particles, and our Stern layer conductance values as shown in the inset in Fig. 2, the crossover now exhibits a shallow maximum, but is still lower than the actual data by a factor of 4. Allowing for a conductivity-dependent ζ potential produces similar results.

Considerable empirical evidence [9–12], particularly for ion-selective conducting particles, suggests that a normal capacitive current, missing in the classical theories, is responsible for the discrepancy seen in Figs. 1 and 2 at the critical region of $\lambda\sim a$. If the migrating ions are allowed to accumulate at the opposite poles, an induced dipole that favors positive dielectrophoresis increases ω_{CO}. If we assume that the diffuse layer permittivity and conductivity are similar to those of the bulk medium, the diffuse layer capacitance would be ε_M/λ and its resistance along the particle a/σ_M. Consequently, we expect ω_{CO} of this theory to scale as the inverse RC time of the diffuse layer,

$$\omega_{DL}\sim\left(\frac{\lambda\sigma_M}{a\varepsilon_M}\right)=\frac{D}{a\lambda}. \tag{2}$$

This simple expression quantitatively captures ω_{CO} for smaller particles, as seen in Figs. 1 and 2. Its ratio to ω_∞, the low-conductivity limiting frequency from the MW theory, is $(1/2\pi)(\sqrt{2}\sigma_M/\sigma_p)(\lambda/a)$, and this ratio increases monotonically with medium conductivity σ_M. As is evident from the 93 nm data in Fig. 1, this scaling can be almost a factor of 10 larger than ω_{MW}.

Our theory, which quantitatively confirms the above scaling, uses Stern layer conduction to describe σ_p, but describes both tangential and normal (conducting and diffusive) fluxes in the diffuse layer explicitly. It follows that of Gonzalez *et al.* for electrode double-layer polarization [12] with a Debye-Hückel linearization for a symmetric monovalent electrolyte, whose dynamic space charge fluctuation and charge density are small compared to the dc ion concentrations. However, Gonzalez *et al.* consider the thin double-layer limit of $(a/\lambda)\gg1$, while we include the full Laplacian for the Poisson equation and for the charge transport equation for $\lambda\sim a$. After a Fourier transform in time, the dimensionless ac components of the charge density ρ (scaled by $2n_0e$), the medium and particle potential (scaled by k_BT/e), the spatial coordinates scaled by a, and the time scaled by (ε_M/σ_M), the two potentials and charge density satisfy

$$\nabla^2\phi_M=-\left(\frac{a}{\lambda}\right)^2\rho,\quad \nabla^2\phi_P=0,$$

$$\nabla^2\rho=\left[\left(\frac{ia^2}{D}\right)\left(\frac{\omega\sigma_M}{\varepsilon_M}\right)+\left(\frac{a}{\lambda}\right)^2\right]\rho=s^2\left(\frac{a}{\lambda}\right)^2\rho, \tag{3}$$

where ω, the dimensionless frequency, has been scaled by (σ_M/ε_M), and the complex number s is defined by $s^2=1+i\omega$. The Laplacian on the left of the charge density represents diffusion, while the two terms on the right represent accumulation and electromigration, respectively.

With a uniform unit dimensionless far field in $\hat{e}_Z$, the relevant axisymmetric charge density solution to the Bessel equation (3) can be expressed as a Bessel function of fractional order, and the particle and medium potentials contain the related spherical harmonics,

$$\rho=\frac{BK_{3/2}\left(\frac{a}{\lambda}sr\right)}{r^{1/2}}\cos\theta,\quad \phi_P=Dr\cos\theta,$$

$$\phi_M=\left(-\frac{BK_{3/2}\left(\frac{a}{\lambda}sr\right)}{s^2r^{1/2}}+\frac{A}{r^2}-r\right)\cos\theta, \tag{4}$$

where the first term in the medium potential represents the polarized space charge distribution in the diffuse layer and the second term represents the field due to the induced particle dipole. As the space charge contribution to the potential decays exponentially as $\exp(-asr/\lambda)$, it is clear from Eq. (4) that the potential seen by any second-order applied field with a finite gradient is predominantly due to the dipole and not

the space charge. We hence do not need to be concerned with the Maxwell force on the space charge, nor the resulting electro-osmotic convection. The space charge is nevertheless important, as it screens the external field such that the particle dipole is different from the unscreened one as for $(\lambda/a) \gg 1$. With negligible space charge contribution to the electric force on the particle, the coefficient A for the complex charge of the induced dipole can be used directly in the classical expression for the dipole force, $4\pi\varepsilon_M \mathrm{Re}(A) a^3 \hat{E}\cdot(\hat{\nabla}\hat{E})$, to obtain the DEP velocity $u_{DEP} = (\varepsilon_M a^2/6\pi\mu)\mathrm{Re}(A)\hat{\nabla}|\hat{E}|^2$, where $\hat{E}$ is the dimensional electric field.

The specific values of A, however, require determination of the coefficients in Eq. (4). The MW theory uses as surface boundary conditions the potential continuity $[\phi]=0$ and the complex displacement continuity in dimensional form,

$$\left[\tilde{\varepsilon}\frac{\partial\phi}{\partial n}\right] = 0 \tag{5}$$

where $[\cdot]$ denotes a jump across the particle surface, and the Stern layer effect is included in the particle conductivity. Equation (5) is derived by eliminating the surface charge q_s from the surface charge accumulation due to the conductive flux imbalance, $i\omega q_s = [\sigma\partial\phi/\partial n]$, and the displacement jump due to the surface charge, $-q_s = [\varepsilon\partial\phi/\partial n]$, where the ac surface charge resides at the diffuse/Stern layer interface. However, an additional boundary condition on this interface is needed for the space charge density ρ. For the normal diffuse layer current to be a charging current, the space charge must adsorb onto the surface.

Adsorption of counterions at the Stern layer has been well documented [13–15], and a reversible adsorption isotherm is usually assumed, as the adsorption and desorption kinetic times across the Stern layer are expected to be on the order of nanoseconds or shorter. This corresponds to an ion association reaction, as the counterion is condensing onto a surface charge of opposite sign, and available quasielastic neutron scattering (QENS) and NMR studies of association time scales ($<10^{-9}$ s) are indeed much shorter than the inverse crossover frequencies of nanocolloids, except for very large hydrated ions [16]. We model this Stern layer of thickness λ_s to have the same conductivity and permittivity as the medium. The adsorbed Stern layer charge σ_s is distinct from the surface charge q_s responsible for the complex MW condition Eq. (5), where q_s is due to smaller charge carriers than the adsorbed ions and exists at the inside (solid) boundary of the Stern layer. We hence exchange the potential continuity equation at the particle surface with the Stern layer condition of a potential jump across the Stern layer, with adsorbed Stern layer charge related to the space charge ρ by an equilibrium isotherm $\sigma_s = K_{eq}\rho$,

$$\phi_P - \phi_M = K'_{eq}\left(\frac{\lambda_S}{\lambda}\right)\rho, \tag{6}$$

where $K'_{eq} = K_{eq}/\lambda$. Accumulation of σ_s in the Stern layer due to imbalance in particle and medium fluxes yields, using the same isotherm, the dimensionless condition

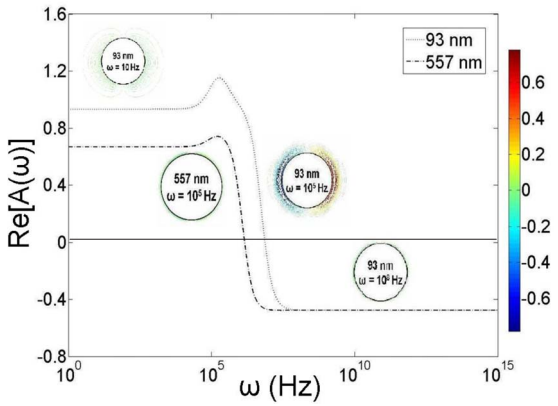

FIG. 3. (Color online) Real part of the dipole strength A for 93 and 557 nm particles for $\sigma_M = 1$ mS m^{-1}, $\lambda = 37$ nm, $K_s = 1.46$ nS for 93 nm particles and $K_s = 1.92$ nS for 557 nm particles, relative permitivities of $\varepsilon_M = 78.5$ and $\varepsilon_P = 2.25$, and $D = 10^{-9}$ m^2/s. The Stern layer parameters are $K'_{eq} = 1.0$, $\varepsilon_m/\lambda_S = 80$ μF cm^{-2}. Charge density contours for representative conditions are shown in the insets.

$$\left(\frac{a}{\lambda}\right)\left(\frac{\lambda}{\lambda_S}\right) i\omega(\phi_M - \phi_P) = \frac{\partial\rho}{\partial r} + \frac{\partial\phi_M}{\partial r} - \frac{\sigma_P}{\sigma_M}\frac{\partial\phi_P}{\partial r}. \tag{7}$$

As the field is the same in the Stern layer and on the medium side, we use (the dimensionless version of) Eq. (5) with Eqs. (6) and (7) on the particle surface to solve for the three complex coefficients in Eq. (4). We use a reasonable value for the equilibrium constant $K'_{eq} = K_{eq}/\lambda = 1$ and the literature value [17] for the Stern layer capacitance $\varepsilon_m/\lambda_S = 80$ μF cm^{-2}. The Stern layer RC time is simply the capacitance term in Eq. (7) and yields a characteristic frequency $\omega_{Stern} = (D/a\lambda)(\lambda_S/\lambda) \ll \omega_{DL}$. With Stern layer adsorption, the diffuse layer also becomes a capacitor. However, since both Stern and diffuse layer capacitors are in series relative to the normal charging current, it is the diffuse layer with lower

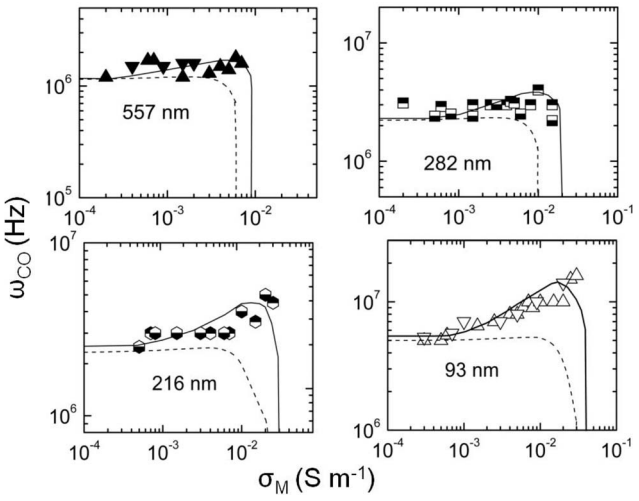

FIG. 4. Comparison of our present theory to Green and Morgan's data using the parameters in Fig. 3. The Stern layer conductance for each particle is given in the inset in Fig. 2. The symbols are the same as in Fig. 2. Dotted curve, MW theory with conducting Stern layer; solid curve, current theory.

capacitance and higher inverse *RC* time that dominates, such that ω_{DL} of (2) captures the data in Figs. 1 and 2.

The coefficients are determined from a series expansion of the complex functions. The real part of the charge density distribution within the diffuse layer is plotted in Fig. 3 for the two particles of Fig. 1 with λ roughly the size of the smaller one. There is negligible space charge in the diffuse layer of the larger particle for all frequencies, as in the MW theory. For the smaller particle, the Stern layer capacitor is saturated at frequencies much lower than ω_{Stern}, and the tangential conduction in the diffuse layer drains the space charge away. At higher frequencies, the ac period is too small for charging current to penetrate the diffuse layer to reach the Stern layer. These limits, hence, correspond to the conductive and dielectric polarization mechanisms of the MW theory, and there is again no space charge. At about $\omega_{Stern} \sim 10^5$ Hz, however, the charge density of the smaller particle becomes dramatically higher due to Stern layer charging. Re$[A]$ is also shown in Fig. 3 for both nanocolloids. While the larger colloid shows a small correction to classical MW dipole intensity that decreases with increasing frequency, a sharp maximum is observed for the smaller particle at a frequency near ω_{Stern}. As shown in Fig. 4, all the crossover frequency data for various particle sizes by Green and Morgan can be captured with this model by using the proper a/λ for each experiment and using the Stern layer conductance obtained from the asymptotic crossover of the latex particles at low medium conductivity. Adjusting the equilibrium constant K'_{eq} and the Stern layer capacitance, the only unknown parameters, over one order of magnitude does not change the curves significantly, provided $\omega_{Stern} \ll \omega_{DL}$.

We thank Z. Gagnon, F. Plouraboue, and H. H. Wei for valuable discussions on this subject and acknowledge financial support from the Center of Applied Math and NSF.

[1] H. Morgan and N. G. Green, *AC Electrokinetics: Colloids and Nanoparticles* (Research Studies Press, Hertfordshire, U.K., 2003).
[2] H. A. Pohl, *Dielectrophoresis* (Cambridge University Press, Cambridge, U.K., 1978).
[3] T. Bellini, F. Mantegazza, V. Degiorgio, R. Avallone, and D. A. Saville, Phys. Rev. Lett. **82**, 5160 (1999).
[4] L. Gorre-Talini, S. Jeanjean, and P. Silberzan, Phys. Rev. E **56**, 2025 (1997).
[5] S. Tsukahara, K. Yamanaka, and H. Watarai, Langmuir **16**, 3866 (2000).
[6] N. G. Green and H. Morgan, J. Phys. Chem. B **103**, 41 (1999).
[7] I. Ermonila and H. Morgan, J. Colloid Interface Sci. **285**, 419 (2005).
[8] J. Lyklema and M. Minor, Colloids Surf., A **140**, 33 (1998).
[9] S. S. Dukhin, Adv. Colloid Interface Sci. **35**, 173 (1991).
[10] Y. Ben and H.-C. Chang, J. Fluid Mech. **461**, 229 (2002).
[11] Y. Ben, E. A. Demekhin, and H.-C. Chang, J. Colloid Interface Sci. **276**, 483 (2004).
[12] A. Gonzalez, A. Ramos, N. G. Green, A. Castellanos, and H. Morgan, Phys. Rev. E **61**, 4019 (2000).
[13] O. Zohar, I. Leizerson, and U. Sivan, Phys. Rev. Lett. **96**, 177802 (2006).
[14] C. S. Mangelsdorf and L. R. White, J. Chem. Soc., Faraday Trans. **94**, 2441 (1998); **94**, 2583 (1998).
[15] P. Takhistov, A. Indeikina, and H.-C. Chang, Phys. Fluids **14**, 1 (2002).
[16] H. Ohtaki and T. Radnal, Chem. Rev. (Washington, D.C.) **93**, 1157 (1993).
[17] R. Guidelli, *Electrified Interfaces in Physics, Chemistry and Biology*, NATO Advanced Study Institute No. 355, Series C: Mathematical and Physical Sciences (Kluwer Academic, Dordrecht, 1992).